

Fractal Analysis of Ultrasound Images of Carotid Atherosclerotic Plaque

P. Asvestas, S. Golemati, G.K. Matsopoulos, and K.S. Nikita

Department of Electrical and Computer Engineering, National Technical University of Athens, GREECE
email: sgolemati@biosim.ntua.gr

Abstract- In this paper, we investigate the possibility of using the fractal dimension to characterise carotid atheromatous plaques from B-mode ultrasound images. The images were obtained from ten symptomatic and nine asymptomatic subjects. Symptomatic subjects included patients with previous history of cerebral events, whereas asymptomatic ones had no evidence of any cerebral symptoms prior to the time of the investigation. For each subject, a sequence of images was collected corresponding to 2-3 cardiac cycles. The boundary of the atheromatous plaque was defined by an expert in three different images of each sequence, corresponding to systole, diastole and a random phase of the cardiac cycle. The fractal dimension of each plaque was estimated using a new method, namely the k -th nearest neighbour method. The results showed that the values of the fractal dimension in the symptomatic group were significantly higher than those in the asymptomatic group. These results suggested that the fractal dimension, estimated from B-mode ultrasound images, could be used to discriminate between symptomatic and asymptomatic carotid atheromatous plaques.

Keywords – B-mode ultrasound, carotid, atherosclerotic plaque, fractal dimension, k th nearest neighbour method

I. INTRODUCTION

Ultrasound imaging of the carotid artery is widely used in the diagnosis of carotid atherosclerosis as it allows non-invasive assessment of the degree of stenosis as well as of plaque morphology, including plaque homogeneity/heterogeneity, plaque echogenicity/echolucency, plaque texture and plaque surface characteristics. It has been demonstrated that the possibility that a carotid plaque produces a cerebral event (symptom), i.e. its instability, may be determined by the degree of stenosis [1], with plaques causing high degrees of stenosis more likely to produce symptoms.

However, carotid plaques with relatively small degrees of stenosis have been reported to cause symptoms. Furthermore, due to the fact that the majority of symptoms occur in previously asymptomatic subjects, it is important to study additional parameters that may contribute to recognise and treat subjects (especially asymptomatic ones) at high risk of cerebral events.

Plaque morphology, determined from ultrasound images of the carotid artery, may be related to the risk of clinical events. Homogeneous plaques are characterised by uniformly high- or medium-level echoes and are associated with stable plaques; heterogeneous plaques are associated with advanced stages of carotid plaque lesion [2]. Echogenic plaques reflect strongly the ultrasound signal, whereas echolucent ones have less reflecting ability. It has been shown that echolucent plaques, as evaluated by B-mode ultrasound, are more likely

to lead to the development of neurological events than echogenic ones [3]. Analysis of digital images of carotid plaques allows assessment of plaque texture. First and second order statistical features extracted from carotid plaques may provide useful information about the correlation between texture and plaque composition [4].

In addition, the texture of biological tissues may be characterised using the fractal dimension [5]. For an image, the fractal dimension is a non-integer number between 2 and 3 and is a measure of the roughness of its intensity surface. Experiments have demonstrated that the fractal dimension is highly correlated with the human perception of image texture; the rougher the texture, the larger the fractal dimension.

In this paper, the fractal dimension was used as a texture feature in order to characterise carotid plaques from B-mode ultrasound images obtained from the two main types of patients with carotid atherosclerosis, namely symptomatic and asymptomatic. A recently proposed method, namely the k th nearest neighbour method, was used for estimating the fractal dimension [6].

II. METHODOLOGY

A. Subjects and Procedures for Acquisition of Images

A total of 17 subjects, who were recruited from patients referred to the Irvine Laboratory, St Mary's Hospital, London for neck arteries scanning, were selected for the study. The above population provided a total of 19 carotid arteries with an atherosclerotic plaque on the vessel wall (for 2 of the investigated subjects both carotid arteries were studied). Among these, 10 plaques were symptomatic (ages 50-85 years, mean 67.9 years, 2 females) and 9 were asymptomatic (ages 50-90 years, mean 67.6, 6 females). Symptoms included stroke, hemispheric transient ischaemic attack and amaurosis fugax. The majority of the investigated plaque regions were located in the internal carotid artery, close to or exactly at the site of the carotid bulb.

For each subject, a scan sequence was recorded with an ATL (Advanced Technology Laboratory) Ultramark 4 Duplex scanner and a high resolution 7.5MHz linear array scanhead. Scanner settings (dynamic range 60dB, 2D grey map, persistence low, frame rate high) were set at the beginning of the recording and not altered during the procedure. These settings were common for all investigations. Carotid arteries were imaged in longitudinal section, as this section provides more information about the vessel wall. The sequences were recorded at a rate of 25 frames/sec for 3 seconds during breathholding. The images

Report Documentation Page

| | | |
|--|--|--|
| Report Date 25 Oct 2001 | Report Type N/A | Dates Covered (from... to) - |
| Title and Subtitle Fractal Analysis of Ultrasound Images of Carotid Atherosclerotic Plaque | | Contract Number |
| | | Grant Number |
| | | Program Element Number |
| Author(s) | | Project Number |
| | | Task Number |
| | | Work Unit Number |
| Performing Organization Name(s) and Address(es) Department of Electrical and Computer Engineering National Technical University of Athens Greece | | Performing Organization Report Number |
| Sponsoring/Monitoring Agency Name(s) and Address(es) US Army Research, Development & Standardization Group (UK) PSC 802 Box 15 FPO AE 09499-1500 | | Sponsor/Monitor's Acronym(s) |
| | | Sponsor/Monitor's Report Number(s) |
| Distribution/Availability Statement Approved for public release, distribution unlimited | | |
| Supplementary Notes Papers from 23rd Annual International Conference of the IEEE Engineering in Medicine and Biology Society, October 25-28, 2001, held in Istanbul, Turkey. See also ADM001351 for entire conference on cd-rom. | | |
| Abstract | | |
| Subject Terms | | |
| Report Classification unclassified | Classification of this page unclassified | |
| Classification of Abstract unclassified | Limitation of Abstract UU | |
| Number of Pages 4 | | |

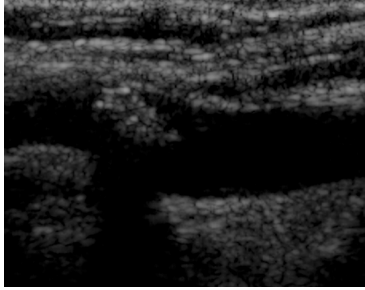
were transferred to a magnet optical disc and then copied to a compact disc. Then they were copied to a personal computer where the analysis was performed.

Each sequence was reviewed and two frames corresponding to diastole and systole were selected by an expert. Furthermore, for each subject, a random frame, namely the first frame, of the sequence was also included in the study. The reason for including a random frame in the study was to examine whether the value of the fractal dimension was dependent on the phase of the cardiac cycle.

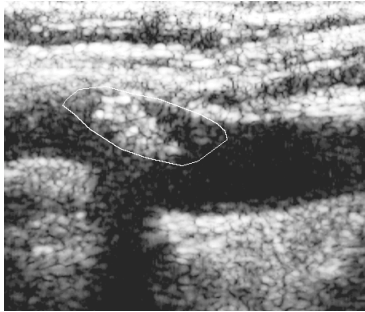
For each of the three selected frames, histogram equalization was performed and the outline of the plaque region was drawn by an expert. Histogram equalization improves visualization of the plaque and thus enables the expert to draw the plaque boundary. The plaque boundary on the histogram equalized image was then applied on the original image to define the region for which the fractal dimension would be estimated. It must be noted that the fractal dimension was estimated for the original image, not the equalized one. Fig. 1 shows a typical example of a frame and its histogram equalized version where the plaque was outlined.

B. The k th-nearest neighbour method

Several methods have been proposed for the estimation of the fractal dimension (FD) of images. In this paper, a method for estimating the fractal dimension, namely the k -th nearest neighbour, was applied. The reason for selecting this method was based on the fact that existing methods for estimating FD



(a)



(b)

Fig 1. Typical example of ultrasound image of a carotid artery (a) and its equalised version (b).

such as the box-counting method [7], underestimate the true fractal dimension for relatively high values (e.g. above 2.6), mainly due to the discretization of the image domain and the quantization of the grey levels. Furthermore, as opposed to other widely used methods (e.g. the power spectrum method), the existence of an underlying model for the available data is not a prerequisite for the proposed method.

The k th nearest neighbour method is the main representative of the so-called fixed - mass methods. In particular, Badii and Politi [8] considered moments of the average distance to the k th nearest neighbour and recommended keeping k fixed and computing a dimension function, $D(\gamma)$, from the scaling of average moments of r_k with the total number of points N as follows:

$$\langle r_k^\gamma \rangle \sim (k/N)^{\gamma/D(\gamma)} \quad (1)$$

It can be shown that fractal dimension is the fixed point of the dimension function, $D(\gamma)$, that is $D(FD) = FD$ [8].

The proposed procedure for the estimation of the fractal dimension of a grey level image, $I(x, y)$, with size $N_x \times N_y$ pixels, using (1), for $k = k_{\min}, \dots, k_{\max}$ (k integer), is as follows:

Step 1. An initial value of γ , γ_0 , is chosen arbitrarily.

Since the fractal dimension of an image is between 2 and 3, it would be better to choose γ_0 in this range, e.g. $\gamma_0 = 2.5$. However, the performance of the method is not affected significantly by the initial value of γ [6].

Step 2. Each pixel of the image with spatial coordinates (x, y) is considered as a point of R^3 with coordinates $(x, y, I(x, y))$. For each such point, which will be referred as a reference point, its k_{\min} up to k_{\max} nearest neighbours are recorded as r_{k_m} ($m = 1, 2, \dots, N$), where $N = N_x \times N_y$ denotes the total number of the pixels in the image.

Step 3. For $n = 1, 2, \dots$ the following recursive relations:

$$D(\gamma_n) = \frac{\gamma_{n-1}}{s_{n-1}} \\ \gamma_n = D(\gamma_n)$$

are applied until convergence is achieved. s_{n-1} is the slope of the best fitting line (using linear regression) at the points $(\log(k/N), \log \langle r_k^{\gamma_{n-1}} \rangle)$ and

$\langle r_k^{\gamma_{n-1}} \rangle = \frac{1}{N} \sum_{m=1}^N r_{k_m}^{\gamma_{n-1}}$. The distance between two points

was determined using the Euclidean norm.

The process can be terminated when the fractional range between γ_{n-1} and $D(\gamma_n)$, $\left| \frac{D(\gamma_n) - \gamma_{n-1}}{0.5[D(\gamma_n) + \gamma_{n-1}]} \right|$, is smaller

than some predefined tolerance (e.g. 10^{-5}). Experiments have shown that just two or three iterations are sufficient for the calculation of the fractal dimension of images [6].

The calculation of the distances of each point from its k th nearest neighbours can be carried out using a fast nearest neighbour search based on binary space partitions (kd-trees, see [9]). To further accelerate the calculation of the distances, an approximate nearest neighbour search [10] can be performed, i.e. only queries for points whose distance is at most $(1 + \varepsilon)$ times larger than the distances of each point from its k th nearest neighbours are considered. Additionally, instead of using all the pixels of the image as reference points, only a number of N_{ref} randomly chosen pixels ($N_{ref} < N$) can be used as reference points for calculating $\langle r_k^\gamma \rangle$, leading to further acceleration without significant loss of the accuracy of the calculation.

III. RESULTS

The values of the fractal dimension (mean value \pm standard deviation) for each of the three investigated frames of each sequence are listed in Table I. The initial value for γ was $\gamma_0 = 2.5$. The range of k values was chosen heuristically to be between $k_{min} = 50$ and $k_{max} = 150$. The parameter ε was set to zero, which means that the distances from the exact nearest neighbours were taken into account and finally all the pixels belonging to the plaque region were used as reference points.

A two-tailed Student's t-test was performed in order to determine whether there was a statistically significant difference between the fractal dimension of the symptomatic and the asymptomatic subjects. The null hypothesis was that the two groups did not differ as per the fractal dimension. The test showed that the null hypothesis could be rejected with significance level $p < 0.01$ (Table I). This finding was independent of the phase of the cardiac cycle. The corresponding 95% confidence intervals for the mean value of the fractal dimension of the plaque region of the two populations are shown in Table II.

TABLE I
FRACTAL DIMENSION FOR SYMPTOMATIC AND ASYMPTOMATIC SUBJECTS

| | Diastole | Systole | Random frame |
|----------------|-------------------|-------------------|-------------------|
| Symptomatic | 2.320 \pm 0.041 | 2.313 \pm 0.078 | 2.303 \pm 0.062 |
| Asymptomatic | 2.159 \pm 0.111 | 2.185 \pm 0.048 | 2.162 \pm 0.093 |
| <i>p-value</i> | 0.000558 | 0.000493 | 0.001080 |

TABLE II
LOWER AND UPPER LIMITS OF THE 95% CONFIDENCE INTERVALS FOR THE MEAN VALUE OF THE FRACTAL DIMENSION OF THE PLAQUE REGIONS FOR THE TWO POPULATIONS.

| | | Systole | Diastole | Random frame |
|--------------|-------------|---------|----------|--------------|
| Symptomatic | Lower limit | 2.257 | 2.290 | 2.259 |
| | Upper limit | 2.369 | 2.349 | 2.348 |
| Asymptomatic | Lower limit | 2.148 | 2.074 | 2.090 |
| | Upper limit | 2.222 | 2.244 | 2.234 |

In order to assess whether there was a difference of the fractal dimension estimations between the different phases, a one-way repeated-measures analysis of variance (RM-ANOVA) was performed [11]. The null hypothesis was that the independent variable (i.e. the phase) had no effect on the estimation of the fractal dimension of the plaque regions.

The results of the test are listed in Table III. The first column of the Table presents the sources of variation of the fractal dimension estimations. One source of variation was the independent variable manipulation (phase): 19 of the estimations were obtained during systole, 19 during diastole and 19 during an arbitrary phase (first frame). Another source of variation was the individual differences: the mean value of the three fractal dimension estimations. The final component of the total variability is due to the so-called phase \times subjects interaction and it describes how the patterns of the fractal dimension estimations of the subjects are affected by the levels of the independent variable (phase).

The quantification of the various sources of variation is achieved by the use of the sum of squares (SS), which is an abbreviation for the "sum of the squared deviations from the mean". The values for the sum of squares for the three components are listed in the second column of the Table III. The third column of the Table III contains the degrees of freedom (df) for each source of variation. The column labelled as MS presents the mean of squares, which is the ratio of the sum of squares to the degrees of freedom. Since the mean of squares corresponding to the second component of variation is not used for further calculations, therefore, it is not necessary to include it in the Table III.

TABLE III
ONE-WAY RM-ANOVA FOR ASSESSING IF THE MEAN VALUES OF THE FRACTAL DIMENSION OF THE PLAQUE REGIONS ARE DIFFERENT BETWEEN THE THREE PHASES.

| Source of variation | SS | df | MS | F | p-value |
|---------------------|---------|----|----------|----------|----------|
| Phase (P) | 0.00247 | 2 | 0.001234 | 0.366728 | 0.695557 |
| Subjects (S) | 0.46450 | 18 | - | | |
| PxS | 0.12114 | 36 | 0.003365 | | |
| Total | 0.58811 | 56 | | | |

The systematic effect of the phase on the fractal dimension estimations is quantified by the so called F-ratio, which is the ratio of the mean squares of the first component of variation to the mean of squares of the third component of variation. The p-value corresponding to the computed F-ratio

(0.695557) indicates that the null hypothesis cannot be rejected. Consequently, the phase had no systematic effect on the estimation of the fractal dimension of plaque regions and the observed differences can be attributed to chance alone.

Furthermore, a well-known algorithm of unsupervised learning, namely the fuzzy c-means algorithm [12], was applied for the clustering of the input data into two clusters. In particular, for each subject, a feature vector was formed using the three values of the fractal dimension estimated during the three phases. Thus, a total of 19 feature vectors were formed, which were the input of the algorithm. On output, the centres of the two clusters (Cluster 1 for the symptomatic subjects and Cluster 2 for the asymptomatic) and the values of the membership function for each vector were obtained. Each vector was assigned to the cluster corresponding to the maximum of its membership function values. All the feature vectors obtained by the asymptomatic subjects formed cluster 2, whereas 9 out of 10 of the feature vectors formed cluster 1. Thus the percentage of correct classification was 94.7%.

V. CONCLUSIONS

In this paper, the fractal dimension of atheromatous plaques of the carotid arteries of two groups of subjects, symptomatic and asymptomatic was estimated. The results indicated a significant statistical difference of the fractal dimension of the plaques extracted from symptomatic and asymptomatic subjects, for both the diastole and the systole as well as for the first frame of the sequence. No significant difference was observed for the inter-phase comparison of the fractal dimension estimations. Therefore, it is concluded that the fractal dimension can be calculated for any phase of the cardiac cycle.

In order to establish the fractal dimension as a determinant of carotid plaque instability, a larger group of both types of plaques should be investigated. This larger-scale study will be based on recruitment of patients according to a pre-defined protocol, in which patient clinical history and procedures for image acquisition are standardised and described in detail. The patients whose plaques are interrogated will then be followed-up at regular intervals in order to determine a subgroup of asymptomatic subjects that will develop cerebral events after the first investigation. The value of the fractal dimension within this subgroup of asymptomatic subjects, if different from that of the rest of the asymptomatic group, will allow the vascular surgeon to select those asymptomatic subjects who need carotid endarterectomy.

ACKNOWLEDGMENT

Special thanks are due to Prof. A. N. Nicolaides at the Irvine Laboratory, St. Mary's Hospital, London, for providing the frame sequences, and identifying the carotid plaque regions of the ultrasound images used in the study.

REFERENCES

- [1] North American Symptomatic Carotid Endarterectomy Trial Collaborators (NASCETC), "Benefit of carotid endarterectomy in patients with symptomatic moderate or severe stenosis," *N. Engl. J. Med.*, vol. 339, pp. 1415-1425, 1998.
- [2] L.M. Reilly, R.J. Lusby, L. Hughes, L.D. Ferrell, R.J. Stoney and W.K. Ehrenfeld, "Carotid plaque histology using real-time ultrasonography. Clinical and therapeutic implications," *Am. J. Surg.*, vol. 146, pp. 188-193, 1983.
- [3] M.-L.M. Grønholdt, "Ultrasound and lipoproteins as predictors of lipid-rich rupture-prone plaques in the carotid artery," *Arterioscler. Thromb. Vasc. Biol.*, vol. 19, pp. 2-13, 1999.
- [4] J.E. Wilhjelm, M.-L. M. Grønholdt, B. Wiebe, S.K. Jespersen, L.K. Hansen and H. Sillesen, "Quantitative analysis of ultrasound B-mode images of carotid atherosclerotic plaque: correlation with visual classification and histological examination," *IEEE Trans. Med. Imaging* vol. 17, pp. 910-922, 1998.
- [5] P. Asvestas, G.K. Matsopoulos and K.S. Nikita, "Application of fractal theory on medical data processing". Section 4, Chapter 3, in *Advanced Infrastructures for Future Healthcare*, A. Marsh, L. Grandinetti, T. Kauranne (Eds.), IOS Press, 2000.
- [6] P. Asvestas, G.K. Matsopoulos and K.S. Nikita, "Estimation of fractal dimension of images using a fixed mass approach," *Patt. Recogn. Letters*, vol. 20, pp. 347-354, 1998.
- [7] N. Sarkar, and B.B. Chaudhuri, "An efficient differential box-counting approach to compute fractal dimension of image," *IEEE Trans. Syst. Man Cybernet.*, vol. 24, pp. 115-120, 1994.
- [8] R. Badii, and A. Politi, "Statistical description of chaotic attractors: the dimension function," *J. Stat. Phys.* vol. 51, pp. 725-750, 1985.
- [9] J.H. Friedman, J.L. Bentley and R.A. Finkel, "An algorithm for finding best matches in logarithmic expected time," *ACM Trans. Math. Softw.*, vol. 3, pp. 209-226, 1977.
- [10] S. Arya, D.M. Mount, N.S. Netanyahu, R. Silverman and A. Wu, "An optimal algorithm for approximate nearest neighbour searching," *Proc. 5th Annu. ACM-SIAM Symp. Discrete Algorithms*, pp. 573-582, 1994.
- [11] N. Furlong, E. Lovelace and K. Lovelace, *Research methods and statistics: an integrated approach*. Harcourt Brace & Company, Orlando, 2000.
- [12] M.R. Rezaee, C. Nyqvist, P.M.J. Van der Zwet, E. Jansen and J.H.C. Reiber, "Segmentation of MR images by a fuzzy c-mean algorithm," *Computers in Cardiology*, pp. 21 - 24, 1995.